SOLIDIFICATION AND MICROSEGREGATION BEHAVIORS OF NICKEL-BASE SINGLE CRYSTAL SUPERALLOY SOLIDIFIED AT MEDIUM COOLING RATE①

Du Wei, Li Jianguo and Fu Hengzhi
State Key Laboratory of Solidification Processing, Northwestern Polytechnical University, Xi'an 710072, P. R. China

ABSTRACT Single crystal blades have already been used in some advanced engines. An industrially valuable nickel-base single crystal superalloy CMSX-2 was solidified at cooling rate from below 1 K/s to 20 K/s. Microstructure and microsegregation were investigated. The results showed that the dendritic arm spacing is highly refined at high cooling rate, the primary dendritic arm spacing can be 35 μm, just as 1/10 as that by conventional HRS processing. With the increase of cooling rate, the microsegregation increases and then decreases. In the superfine columnar dendrite, the γ′ precipitates are very fine; the amount of γ/γ′ eutectic is much fewer and its size is very small.

Key words single crystal superalloy cooling rate microstructure microsegregation

1 INTRODUCTION

Single crystal superalloys are extensively used for advanced high temperature gas turbine. The conventional single crystal superalloy is produced by HRS processing. Because the solid-liquid interface thermal gradient (G_l less than 80 K/cm) and the growth rate (V less than 70 μm/s) are very low[1]. The microstructure of the material is coarse dendrite (λ_1 = 300~400 μm) with well developed side-branches and the segregation is serious. The lower thermal gradient can also cause defects such as freckles, low angle boundaries and porosity[2] which restrict the further improvement in mechanical properties. Dendrite spacing also have a significant influence on mechanical properties, because solidification under high thermal gradient can improve the cooling rate and refine the dendrite, and it is known to be particularly useful in reducing these defects which adversely affects the high temperature strength of the materials. Studies on the different single crystal casting processes have shown that high thermal gradient can overcome these defects and refine the dendritic microstructure[3]. High thermal gradient directional solidification equipment has much higher thermal gradient(200~300 K/cm) than that of the conventional HRS processing. In this paper nickel-base single crystal superalloy specimens was solidified at the cooling rates from below 1 K/s to 20 K/s. Microstructure and microsegregation were investigated.

2 EXPERIMENTAL PROCEDURE

An industrially valuable single crystal superalloy CMSX-2 was chosen for the present study, nominal composition of the alloy is Ni-8Cr-4.6Co-8W-0.6Mo-5.6Al-1Ti-6Ta. Single crystal bulk prepared by the spiral selection method in a directional solidification furnace and cut the seed of d 7 mm × 20 mm from the bulk. The growth direction was within 10° of the [001] orientation of the FCC nickel based gamma matrix. The crucibles are made of high purity alumina. Single crystal bars of d 7 mm × 100 mm were made by the seed method in the self-made

① Project supported by the Aeronautical Science Foundation of China Received May 12, 1997; accepted Jul. 21, 1997

high thermal gradient directional solidification device. Directional solidification was carried out at the constant thermal gradient of 250 K/cm and withdraw speeds varying from 0.01 mm/s to 1 mm/s. The specimens were metallographically polished and etched. Microstructures of the specimens were investigated by an optical microscope, dendritic arm spacing and volume fraction of γ/γ′ eutectic were measured on the transverse section by a Quantimet 500 image analysis system. The number of primary dendritic arm spacing n in a known area A was counted and the primary dendritic arm spacing was calculated as $\lambda_1 = (A/n)^{0.5}$. The volume fraction of γ/γ′ was obtained by analyzing numerous separate field. The second dendrite arm spacing was measured on the longitudinal section within the mushy zone.

Electron probe microanalysis (EPMA) was used to analyze the composition of the dendrite trunk and the inter-dendrite area. The scanning electron microscope was used to investigate the morphology of the γ′ precipitation and γ/γ′ eutectic.

3 RESULTS AND DISCUSSION

3.1 Microstructure

3.1.1 Dendritic arm spacing

Fig. 1 shows the dendritic structure on the transverse section of single crystal superalloy CMSX-2 solidified at different cooling rate. It can be seen that with the increase of cooling rate, dendritic arm spacing were greatly refined. When the cooling rate was higher than 15 K/s, superfine dendritic structure was obtained. The primary dendritic arm spacing λ_1 can be produced to be 35 μm, just as 1/10 as that by HRS processing.

Some analytical models of the dependence of primary dendritic arm spacing on the solidification parameters (thermal gradient G_1 and the solidification rate V) in binary alloy have been proposed[4]. Hunt gave the following relationship for λ_1:

$$\lambda_1 = A G_1^{-0.5} V^{-0.25} \quad (1)$$

The secondary dendritic arm spacing λ_2 predicted by the analytical model is described as the following

$$\lambda_2 = B(G_1 V)^{-1/3} \quad (2)$$

where A and B are constants dependent on the composition of the alloy. Eqn. (3), (4) are the linear least-squared fit to the experimental date.

$$\lambda_1 = -0.00605 + 0.0835 G_1^{-0.5} V^{-0.25} \quad (3)$$

$$\lambda_2 = 0.000855 + 0.00275 (G_1 V)^{-1/3} \quad (4)$$

High value of correlation coefficients, 0.97 and 0.98, and very low value of relative standard deviation for the fit, 4% and 3%, show that the experimental data have an excellent fit

Fig. 1 Dendritic microstructures at different cooling rates

(a) —$G_1 V$ = 0.25 K/s; (b) —$G_1 V$ = 2.5 K/s; (c) —$G_1 V$ = 15 K/s

to the analytical prediction.

3.1.2 Morphology of γ' precipitation

Fig. 2 shows the morphologies of γ' particles transformed with different solidification cooling rate. With the increase of cooling rate, the size of γ' particles decreased, and the γ' particles in the dendritic trunk is smaller than that in the inter-dendrite area. Most of the γ' phase $Ni_A(Al, Ti)$ precipitated from the supersaturating solid solution after solidification and they have the FCC structure and close match to the γ-Ni matrix. In the coarse dendrite which formed at lower cooling rate, the nucleation supercooling and the number of nucleus are small, but the coarsing time is longer. Therefore the size is larger and the shape is irregular. When solidified at higher cooling rate, the nucleation supercooling is higher, large quantity of nucleus is formed, but the growth time decreases, the size of the γ' precipitation is small and the shape is regular cubic. It is found that, when the cooling rate is higher than 15 K/s, the cubic γ' transforms to spherical γ' which results from the initial γ' being spherical[5], at the very high cooling rate, it has not enough time to be coarse and its shape keeps spherical.

3.1.3 Morphology of γ/γ' eutectic

The eutectic consists of large primary γ' bulk, as shown in Fig. 3(a), which is difficult to eliminate by homogenization. In the fine dendrite solidified at higher cooling rate, the amount of γ/γ' eutectic is high and the shape is well developed, the eutectic is screen-like or lamellar, the eutectic cap is still large and consists of coarse γ' phase, as shown in Fig. 3(b). When the cooling rate reaches 15 K/s or larger, in the superfine dendrite, the amount of eutectic is fewer, both dendritic and primary γ' are refined; the eutectic structure is fine and lamellar arrangement is shown in Fig. 3(c). This kind of

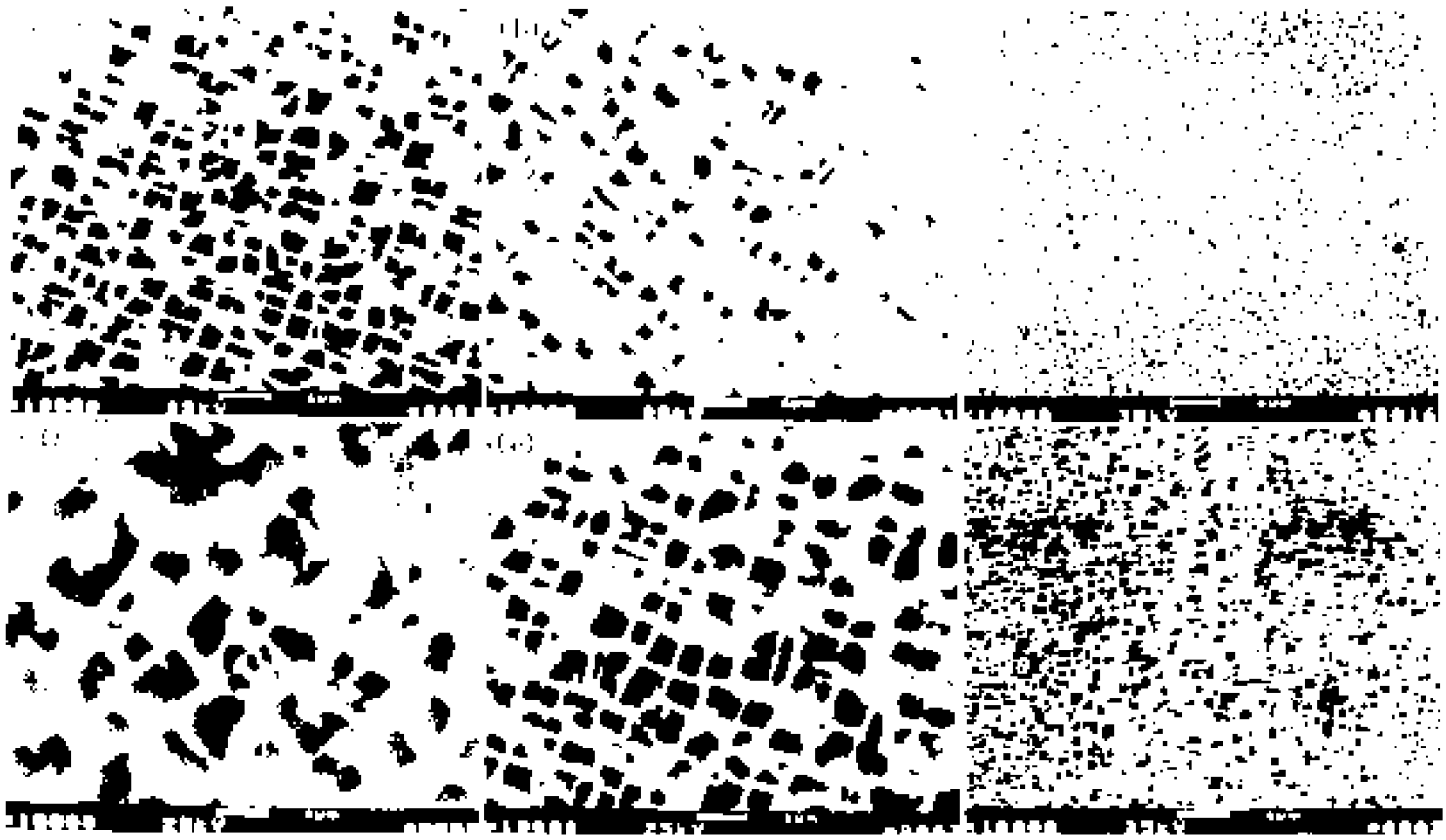

Fig. 2 Morphologies of γ' precipites at different cooling rates

(a), (b), (c) —in dendrite trunk; (d), (e), (f) —in interdendrite area

(a) —G_1V= 0.25 K/s; (b) —G_1V= 2.5 K/s; (c) —G_1V= 15 K/s;

(d) —G_1V= 0.25 K/s; (e) —G_1V= 2.5 K/s; (f) —G_1V= 15 K/s

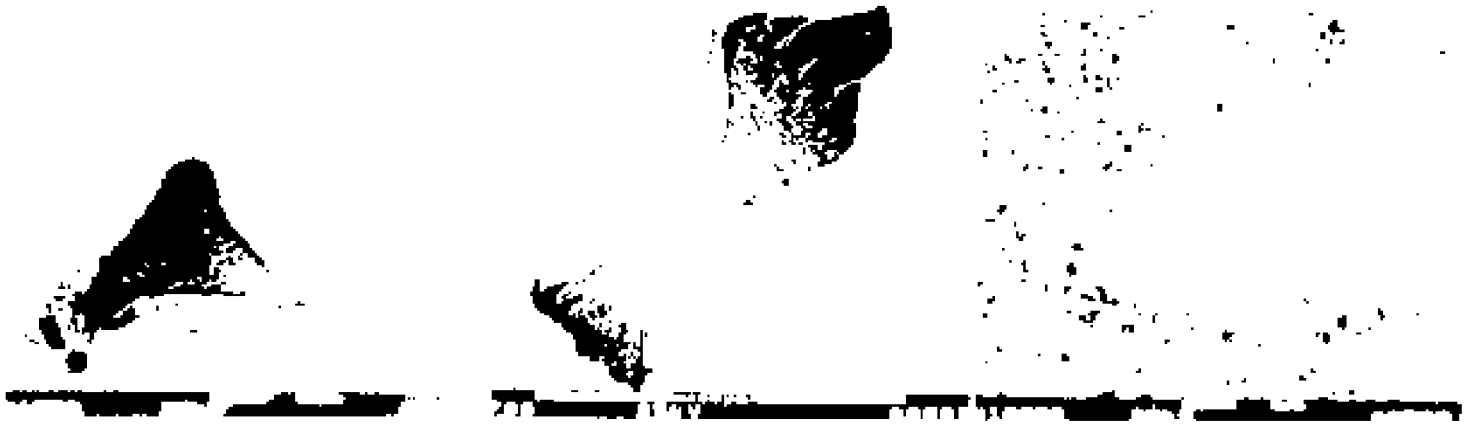

Fig. 3 Morphologies of γ/γ′ eutectic at different cooling rates
(a) $-G_1V$= 0.25 K/s; (b) $-G_1V$= 2.5 K/s; (c) $-G_1V$= 15 K/s

eutectic structure is easy to eliminate by high temperature solution treatment.

Fig. 4 shows the relationship of the amount of γ/γ′ eutectic vs cooling rate, with the increase of cooling rate, the amount of eutectic increases and then decreases. When the cooling rate is lower than 7.5 K/s, the amount of γ/γ′ eutectic increases with the increase of cooling rate, and the size is increasing. In the coarse dendrite solidified at lower cooling rate, the eutectic is fewer but bigger in size.

When the alloy solidified with a dendritic interface, there is a mushy zone in the solidification interface, the elements Al, Ti enriched in the interdendritic area, as the composition of the remaining liquid reaches the eutectic composition, the γ/γ′ eutectic is formed. At low cooling rate the mushy zone is very large, and the more liquid remained which consists of much more solute elements. Consequently, coarse eutectic with large primary γ′ blocks are formed. At high cooling rate, the very fine dendrite divides the remaining liquid into very small melting pool. The microsegregation and the development of the eutectic are restrained, the size and proportion of γ/γ′ eutectic are considerably decreased, the blocky γ′ phase has almost completely disappeared. (see Fig. 3(c)).

3.2 Microsegregation

The results of electron probe microanalysis of alloy elements showed that Cr, Al, Ti, Mo, Ta are depleted and W is enriched in the dendrite core region. Therefore Cr, Al, Ti, Mo, Ta are positive segregation elements and W is the negative segregation element. Fig. 5 shows the relationship of microsegregation ratio(SR) vs cooling rate. It can be known that with the increase of cooling rate, SR increases and then decreases, and each element changes discordantly. This kind of segregation phenomenon might be caused by the following factors:

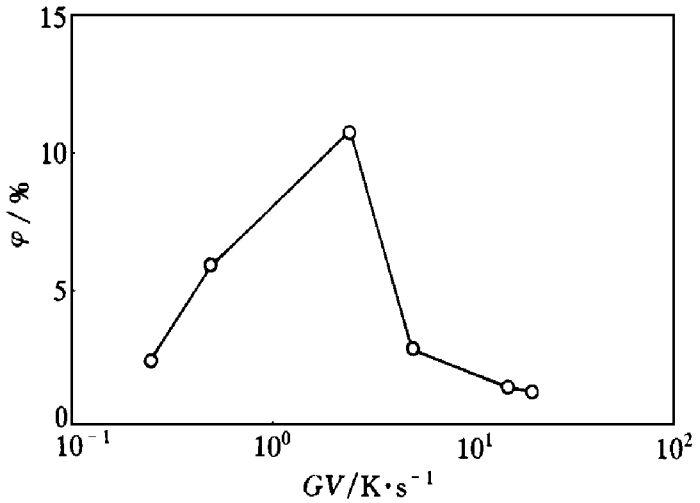

Fig. 4 Amount of γ/γ′ (volume fraction φ) vs cooling rate

(1) The partitioning coefficient (k_i) of each element is different. The partitioning coefficients of Cr, Al, Ti, Mo, Ta are lower than 1 while that of W is higher than 1. The value of the k_i is different, the higher the segregation coefficient ($1 \sim k$) is, the higher the segregation

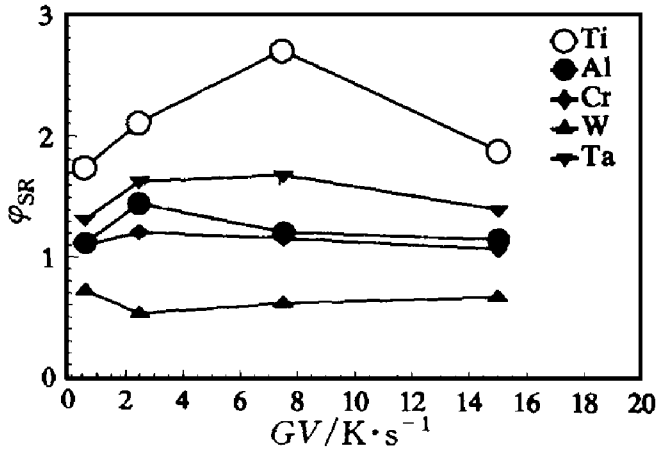

Fig. 5 Segregation ratios(volume fraction ϕ_{SR}) vs cooling rates

○—Tc; ●—Al; ◆—Cr; ▲—W; ▼—Ta

degree is[6].

(2) With the increase of solidification rate, the insufficient back diffusion in the solidified solid causes the increase of microsegregation.

(3) When the solidification rate is much higher, the nonequilibrium effect is much more severe and the partitioning coefficient tends to be concordant[7, 8], which results in suppressed microsegregation.

The amount of eutectic also indicated the degree of microsegregation, apparently the transmutation tendency of the eutectic and the microsegregation is similar.

4 CONCLUSIONS

(1) With the increase of cooling rate, dendritic arm spacing is greatly refined, the relationship of dendritic arm spacing vs cooling rate are

$$\lambda_1 = -0.00605 + 0.0835 G_1^{-0.5} V^{-0.25}$$

$$\lambda_2 = 0.000855 + 0.00275 (G_1 V)^{-1/3}$$

the primary dendritic arm spacing can be produced to be 35 μm, just as one-tenth as that by HRS processing.

(2) With the increase of cooling rate, the γ' precipitates are significantly refined, and the amount of γ/γ' eutectic increases and then decreases. In the superfine columnar dendrite, the γ' precipitates are very fine, the amount of γ/γ' eutectic is much fewer and its' size is very small.

(3) The microsegregation increases and then decreases. In the superfine columnar dendrite, the microsegregation is greatly suppressed, and this is benefit for the homogenization treatment.

REFERENCES

1 Khan T. In: Betz W, Brunetaud R, Couts Ouradis D eds, High Temperature Alloys for Gas Turbine and Other Application. Holland: Reidel D Publishing Company, 1986.

2 Harris K, Erickson G L and Schwer. In: Betz W, Brunetaud R, Couts Ouradis D eds, High Temperature Alloys for Gas Turbines and other Applications. Holland: Reidel D Publishing Company, 1986: 709 – 782.

3 Pollock T M, Murphy W H and Goldman E H. In: Antolovich S D *et al* eds. TMS, 1992: 125– 134.

4 Hu Hanqi. Fundamental of Metal Solidification, (in Chinese). Beijing: Mechanical Industry Publishing, 1991: 93– 100.

5 Guo Xiping. Ph D thesis, (in Chinese). Northwestern Polytechnic University, 1992: 32.

6 Aziz M J. J Appl Phys, 1982, 53(2): 1158.

7 Kurz W, Giovanola B and Trivedi R. Acta Metall, 1986, 36: 823.

8 Sarrel J A, Abbaschian G J. Metal Trans, 1986, 17a: 2063.

(Edited by Huang Jinsong)